

# Development and Applications of Flexible Piezoelectric Nanogenerators Using BaTiO<sub>3</sub>, PDMS, and MWCNTs for Energy Harvesting and Sensory Integration in Smart Systems

Islam Uddin Shipu<sup>\*</sup>, Dipasree Bhowmick<sup>\*\*</sup>, Nondon Lal Dey<sup>\*\*\*</sup>

<sup>\*</sup>Department of Chemistry, The University of Texas Rio Grande Valley, 1201 W University Drive, Edinburg, TX-78539, USA

<sup>\*\*</sup>Department of Mechanical Engineering, The University of Texas Rio Grande Valley, 1201 W University Drive, Edinburg, TX-78539, USA

<sup>\*\*\*</sup>Department of Physics, University of Louisiana at Lafayette, 104 E University Ave, Lafayette, LA-70504, USA

DOI: 10.29322/IJSRP.14.06.2024.p15019  
10.29322/IJSRP.14.06.2023.p15019

Paper Received Date: 03rd May 2024  
Paper Acceptance Date: 06th June 2024  
Paper Publication Date: 15th June 2024

**Abstract-** Mechanical energy is a versatile and accessible green energy source, increasingly harnessed to power small-scale devices via innovative flexible piezoelectric nanogenerators (F-PNGs). These devices convert mechanical energy into electricity using lightweight materials such as Barium Titanate (BaTiO<sub>3</sub>), poly dimethyl siloxane (PDMS), and multi-walled carbon nanotubes (MWCNTs). In this design, BaTiO<sub>3</sub> nanoparticles were embedded in a composite film with PDMS and MWCNTs, sandwiched between two copper electrodes. The BaTiO<sub>3</sub>/PDMS/MWCNT composite PENGs, synthesized for this study, produce an output voltage of ~8 V through periodic cyclic beating. This represents an increase of about 16% compared to the PENGs without MWCNT doping. Additionally, the short-circuit current peaks at about 5.22  $\mu$ A at the optimal MWCNT wt.%. The electrical energy produced can be efficiently captured by a 0.1  $\mu$ F energy storage capacitor, which is then used to power two commercial red LEDs. These findings suggest that the BaTiO<sub>3</sub>/PDMS/MWCNT composite holds significant promise as a lead-free piezoelectric nanogenerator for widespread application.

**Index Terms-** Flexible piezoelectric nanogenerator, Mechanical energy, Energy harvesting, Barium Titanate (BaTiO<sub>3</sub>), Poly Dimethyl Siloxane (PDMS), Multi-Walled Carbon Nanotubes (MWCNTs).

## I. INTRODUCTION

The swift depletion of fossil fuel reserves, coupled with the consequent environmental pollution, has spurred an intensive search for alternative, sustainable energy sources. The emergence of piezoelectric nanogenerators [1] and triboelectric nanogenerators [2] marked a significant milestone in this quest. These technologies have garnered substantial interest due to their

potential to develop highly efficient energy-harvesting devices. By harnessing common mechanical energy sources—such as acoustic waves, fluid motion, body movements, compression, and vibrations—these nanogenerators can effectively convert mechanical energy into electrical power, offering a promising solution for green energy generation [3-5].

Polymers, both synthetic and organic, that possess enough elasticity to react to mechanical pressure are considered ideal for incorporating piezoelectric particles. Among these polymers, flexible polydimethylsiloxane (PDMS) is particularly notable due to its chemical stability, low glass transition temperature, ease of processing, and long-term durability after curing. As a result, PDMS has become one of the most commonly used polymers in nanogenerator design [6–10]. Additionally, lead-free piezoelectric perovskite-type barium titanate (BaTiO<sub>3</sub>) is an excellent choice, providing both environmental safety and a high piezoelectric coefficient [6] [9] [11]. Piezoelectricity arises when certain materials, such as ferroelectrics, undergo a change in polarization in response to mechanical stress [12]. Piezoelectric devices have the capability to harness energy by converting ambient vibrations and strains into electricity [12].

In 1880, Pierre and Jacques Curie conducted experiments to investigate the impact of pressure on the electrical properties of crystals. They discovered that specific crystals, like quartz and tourmaline, generate electric charges on their surfaces when subjected to mechanical stress. This groundbreaking finding demonstrated the conversion of mechanical strain into electrical energy [13]. The Curie brothers further examined the properties of piezoelectric materials and developed the mathematical framework to explain the piezoelectric effect. They introduced the concept of the direct piezoelectric effect, where mechanical stress directly produces an electric charge. They also discovered the converse piezoelectric effect, where an applied electric field causes mechanical deformation in the material [13] [14] [15].

In 1919, a professor introduced an innovative idea involving the use of an amplifier and a crystal in a crystal oscillator control to achieve the desired frequency. This advancement was later applied during World War II to establish communication between aircraft and tanks [16]. Between 1940 and 1970, the ferroelectric dipole properties of Rochelle salt, BaTiO<sub>3</sub>, and LiNbO<sub>3</sub> were uncovered, resembling those of quartz crystal [16]. In 2006, Dr. Z. L. Wang achieved a milestone by developing the inaugural nanogenerator utilizing zinc oxide [17] [18].

For over a decade, there has been an ongoing and vigorous effort to maximize every volt of output power from nanogenerators, while also striving to achieve additional advantages such as lightness, ease of large-scale production, and low cost of the final product. The performance output of a nanogenerator based on polymer composites is influenced by numerous factors, which can be adjusted to enhance efficiency. These factors include the qualitative and quantitative composition of the materials, the uniformity of filler distribution [19,20], chemical doping [21-25], the morphology of the particles [26,27], and the three-dimensional spatial arrangement of particles within the matrix [28-31].

Regarding morphology, research by Jian et al. [20] achieved an output power value of 260 V for a PDMS-based system using hierarchical barium titanate (BTO) flowers. This high output was attributed to the significant local stress at the petals. In contrast, for BTO in the form of nanoparticles [26], nanowires [27], and nanocubes [19], the output values were 3.2 V, 7 V, and 126.3 V, respectively. Chemical doping has proven to be an effective method for modifying the piezoelectric coefficients of materials, thereby enhancing their energy-harvesting capabilities [21-25]. Additionally, the efficiency of load transfer can be improved by creating three-dimensional (3D) structures such as foams [28], porous aerogels [29, 30], and sponge-like configurations [31]. Furthermore, hybrid nanogenerators, which leverage both triboelectric and piezoelectric effects, have shown improved output characteristics, demonstrating the potential for even greater efficiency and performance [32-34].

The creation of a piezoelectric nanogenerator involves utilizing various piezoelectric materials, including nanocomposites, nanofillers, and the polymer poly(vinylidene fluoride) (PVDF). PDMS is a flexible, biocompatible polymer that has gained popularity in nanogenerator fabrication due to its mechanical properties and ease of processing. When combined with piezoelectric materials, PDMS can form composite structures that are both flexible and efficient in energy conversion [35]. PVDF is a semicrystalline polymer made up of repeating CH<sub>2</sub> – CF<sub>2</sub> units. One significant advantage of PVDF film is its flexibility, which allows it to endure stress or pressure on its surface. PVDF is sometimes combined with nanofillers like Fe<sub>3</sub>O<sub>4</sub>, known for its excellent dielectric properties and magnetic behavior [36] [37] [38]. Multiple research groups have demonstrated piezoelectric samples using various materials. One study synthesized three different PVDF samples: PVDF with reduced graphene oxide (RGO), PVDF with NaNbO<sub>3</sub>, and PVDF with both RGO and NaNbO<sub>3</sub>. All samples exhibited the β-phase, but their voltage outputs varied [39]. Another study described synthesizing Fe<sub>3</sub>O<sub>4</sub> from iron (III) acetylacetonate and oleic acid, which was then combined with PVDF to create a PVDF/iron oxide sample. This sample generated a voltage of 35 MV/m when subjected to a

regular force [40]. Furthermore, a study found that ytterbium (III) salt's self-polarization properties enhanced the ferroelectric characteristics of PVDF films [41].

Another important nanofiller, BaTiO<sub>3</sub>, is a ferroelectric material known for its excellent piezoelectric properties, making it a prime candidate for nanogenerator applications [42]. Recent studies have focused on optimizing the synthesis and structural properties of BaTiO<sub>3</sub> to enhance its energy harvesting capabilities. Meisak et al. demonstrated that nanostructured BaTiO<sub>3</sub> exhibits enhanced piezoelectric coefficients due to the increased surface area and reduced grain size, which improve the material's responsiveness to mechanical stress [42]. Additionally, the incorporation of BaTiO<sub>3</sub> nanoparticles into composite matrices has been shown to significantly boost the performance of nanogenerators [42]. Researchers have explored various methods to incorporate PDMS with BaTiO<sub>3</sub> to create flexible nanogenerators. For instance, Bouhamed et al. developed a PDMS-BaTiO<sub>3</sub> composite film that exhibited high durability and efficient energy harvesting capabilities under mechanical deformation. The synergy between PDMS's flexibility and BaTiO<sub>3</sub>'s piezoelectric properties makes these composites ideal for wearable and flexible electronic applications [43]. MWCNTs are renowned for their exceptional electrical conductivity and mechanical strength. When used in nanogenerators, MWCNTs can enhance the electrical output and structural integrity of the devices. The integration of MWCNTs with BaTiO<sub>3</sub> and PDMS has led to significant advancements in the performance of nanogenerators.

Nanofillers are employed to boost the electrical output of nanogenerators when they are subjected to stress. Examples of nanofillers include polyethylene glycol (PEG), carbon-black, and carbon nanotubes, each contributing different benefits. Carbon-black is effective at distributing electricity over long distances but is only useful in the γ-phase [44] [45] [46]. Carbon nanotubes offer excellent dielectric properties, though they are more challenging to handle compared to other nanocomposites [47]. The aim of the current experiment is to create an optimized nanogenerator that enhances the self-polarization of PVDF, thereby increasing the dipole moments and producing a higher electrical charge. Achieving this requires the nanogenerator to reach the β-phase, known for its significant polarization and unique zig-zag structure, which distinguishes it from the other crystalline phases (α, β, γ, δ, ε) [48] [49]. Nanofillers are utilized to help form an organized and crystalline structure in the β-phase, thereby stabilizing the piezoelectric properties of PVDF [39].

In this research, we employed the solid-state synthesis technique to fabricate BaTiO<sub>3</sub> nanoparticles. These nanoparticles were then integrated with MWCNT and embedded into a PDMS polymer matrix to develop a flexible composite film exhibiting piezoelectric properties. To construct a flexible piezoelectric nanogenerator (PENG), copper tapes were adhered to both surfaces of the film, with copper wires serving as extensions. The PENG was subjected to testing across a range of load frequencies, yielding a peak open circuit voltage of approximately 8V and a short circuit current of 5.22μA under periodic cyclic stress. Additionally, the device effectively charged a 0.1μF capacitor, achieving a voltage increase to 6.3V. The PENG also demonstrated successful integration with conventional electronic devices. Overall, this device represents significant progress in the

field of piezoelectric energy harvesting and self-powered sensory technologies.

## II. EXPERIMENTAL PROCEDURE

### A. BaTiO<sub>3</sub> Nanoparticles Synthesis

A conventional solid-state synthesis method was used to prepare BaTiO<sub>3</sub> nanoparticles, utilizing TiO<sub>2</sub> nanoparticles and BaCO<sub>3</sub> nanopowder [50]. To begin, the starting materials were accurately weighed to achieve the correct stoichiometric ratios and then subjected to ball-milling in pure ethyl alcohol for 12 hours using a planetary ball mill. Following the milling process, the mixture was dried at 80°C for 12 hours and subsequently calcined at 1350°C for 4 hours [50].

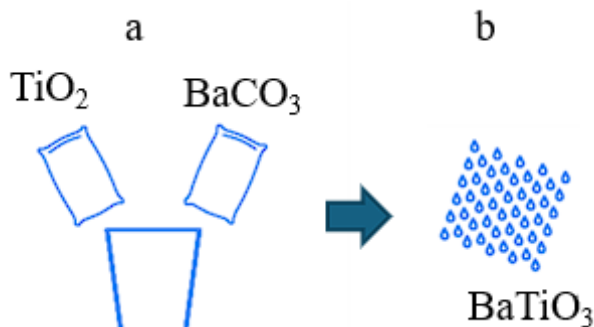


**Fig. 1:** (a) Schematic illustration of the synthesis of BaTiO<sub>3</sub> NPs via a solid-state procedure and (b) Synthesized BaTiO<sub>3</sub> nanoparticles.

### B. Manufacturing of PDMS-BaTiO<sub>3</sub>-MWCNTs Composite Films and F-PENG

The fabrication process for the BaTiO<sub>3</sub>-PDMS-MWCNTs composite thin film can be outlined as follows: Initially, a solution of polydimethylsiloxane (PDMS, Sylgard 184, Dow Corning Corp., Auburn, MI) was prepared by mixing the base with a curing agent in a 10:1 weight ratio. Subsequently, synthesized BaTiO<sub>3</sub> nanoparticles (30 wt.%) and MWCNTs (ranging from 0 to 4.5% relative to the PDMS matrix) were incorporated into the PDMS matrix. The mixture was then stirred magnetically for one hour to ensure the nanoparticles and MWCNTs were evenly dispersed within the PDMS. After initial stirring, the mixture was further agitated at 700 rpm for three hours and ultrasonicated for five minutes at the end of each hour. Afterward, the solutions were placed in a vacuum chamber for 30 minutes to eliminate any bubbles. Then the blend was poured into a glass petri dish and allowed to dry at 80°C for two hours. Following drying, the cured composite film was removed from the glass, cut into 2x2 cm squares, and used in the construction of the F-PENG. The fabrication of the F-PENG involved sandwiching the composite film between two copper electrodes and securing it with Kapton tape to enhance flexibility and durability. This setup was designed to withstand various environmental conditions. Finally, the ideal percentage of MWCNTs was determined by evaluating the electrical output of the film.

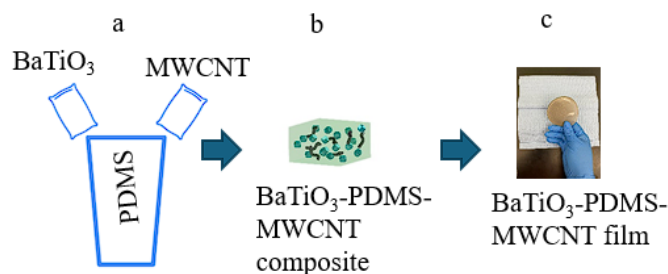


**Fig. 2:** (a-c) BaTiO<sub>3</sub>/MWCNT/PDMS film synthesis.

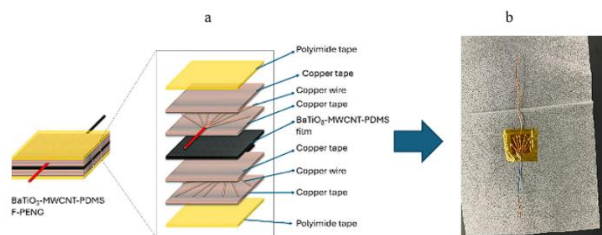


**Fig. 3:** (a,b) F-PENG Fabrication.

## III. RESULTS AND DISCUSSION

Figure 4 presents a scanning electron microscopy (SEM) image of the synthesized BaTiO<sub>3</sub> material, revealing a cluster of nanocrystals with a perovskite-type tetragonal structure. This observation offers valuable insights into the structural characteristics and morphology of the BaTiO<sub>3</sub> crystals, showcasing their unique arrangement and size distribution. The SEM image visually represents the synthesized BaTiO<sub>3</sub> material, aiding in the comprehension of its physical properties and potential applications in various fields.

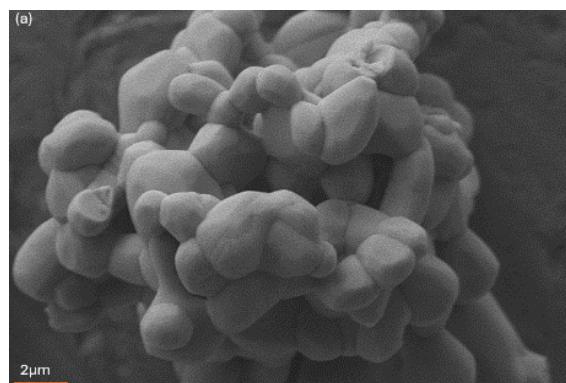


**Fig. 4:** BaTiO<sub>3</sub> NP SEM

The relationship between BaTiO<sub>3</sub> concentration and its output performance is illustrated in Figure 5. The output voltages of approximately 0.73, 1.77, 3.22, 6.79, and 4.11 V were observed from the PNGs for BaTiO<sub>3</sub> nanoparticle fractions of 12, 20, 25, 40,

and 50 wt.%, respectively, during the cycle beating process at a constant force. The data indicates that the output voltage increases progressively with the BaTiO<sub>3</sub> NP content up to 40 wt.%, reaching a maximum of around 6.79 V. However, beyond 40 wt.%, the voltage output decreases, with a recorded value of 4.11 V at 50 wt.%.

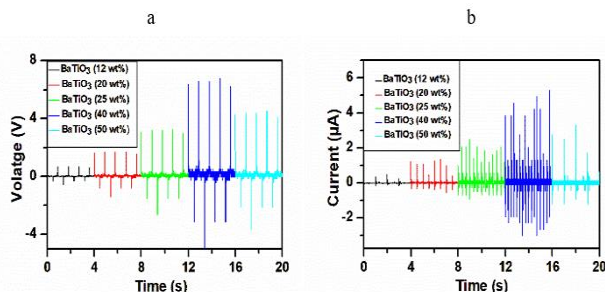


**Fig. 5:** The output performance for BaTiO<sub>3</sub>/PDMS F-PENGs: (a) The output voltage of F-PENGs with 12, 20, 25, 40 and 50 wt.% BaTiO<sub>3</sub> NPs concentration; (b) The output current of F-PENGs with different concentration of BaTiO<sub>3</sub> NPs (12, 20, 25, 40, and 50 wt.%).

Similarly, as shown in Figure 5a, the current peak values differ by approximately 0.45, 1.27, 2.22, 4.34, and 2.79 µA as the BaTiO<sub>3</sub> NP concentration increases from 12 wt.% to 50 wt.%. The current also shows a peak at 40 wt.% before decreasing at higher concentrations.

This trend can be explained by the distribution and density of BaTiO<sub>3</sub> NPs within the PDMS matrix. Up to 40 wt.%, the BaTiO<sub>3</sub> NPs are well distributed, enhancing the material's ability to generate higher voltages and currents. However, beyond this concentration, slight agglomeration of BaTiO<sub>3</sub> NPs occurs, leading to less efficient distribution and interaction within the matrix. This agglomeration reduces the effective surface area and the overall efficiency of the composite, causing a decrease in both voltage and current outputs at higher concentrations.

Therefore, the optimal parameters for PENGs were determined to be a BaTiO<sub>3</sub> NPs concentration of 40 wt.%. For the subsequent step, the film thickness was set at 220 µm.

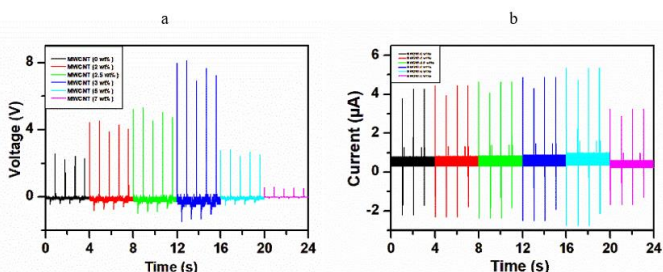


**Fig. 6:** Voltage (a) and current (b) output of different wt.% MWCNT incorporated BaTiO<sub>3</sub>/PDMS F-PENG.

Figure 6 illustrates the time-dependent output voltages for various MWCNT concentrations in PENGs containing 40 wt.% BaTiO<sub>3</sub> NPs during a cyclic beating process. The output voltages obtained were approximately 2.59, 4.42, 5.17, 7.89, 2.76, and 0.56 V for MWCNT fractions of 0, 2, 2.5, 3, 5, and 7 wt.%, respectively (Fig. 6a). It was observed that the voltage increased from 2.59 V (0 wt.% MWCNT) to a peak of 7.89 V (5 wt.% MWCNT) before

dropping to 0.56 V at 7 wt.% MWCNT. The output current displayed a similar trend with varying MWCNT content, reaching as high as 5.22 µA at 5 wt.% MWCNT, as depicted in Fig. 6b. The Carbon nanotubes (CNTs) are made up of sp<sup>2</sup> carbon atoms arranged in tubular structures, resembling rolled-up graphene sheets. They possess exceptional mechanical and electrical properties due to the strong carbon-carbon double bonds and the extensive π-conjugated system. These unique attributes make CNTs ideal multifunctional materials for applications demanding lightweight, flexibility, mechanical strength, and high electrical conductivity [51].

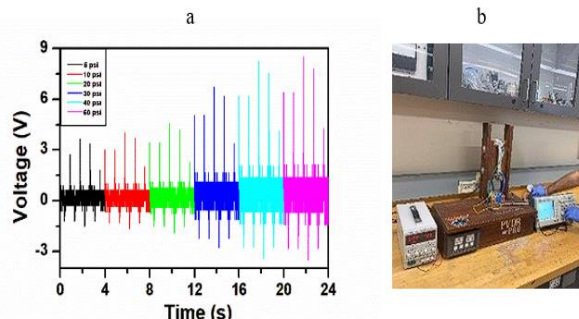


**Fig. 7:** Pressure sensitivity test of F-PENG (a) using an oriental motor (b).

The final F-PENG was tested with varying applied forces using an oriental motor, while maintaining a 10-inch tapping distance. The open circuit voltage (Figure 7) was recorded, revealing maximum output voltages at different force levels: 2.7 V, 3.2 V, 4.9 V, 6.73 V, 8.2 V, and 8.4 V for 5, 10, 20, 30, 40, and 60 psi, respectively, with the peak output occurring at 50 psi. As the force applied to the piezoelectric nanogenerator increases, greater deformation and compression of the material occur, leading to higher voltage outputs through the piezoelectric effect.

The F-PENG's ability to sense body motion was assessed through tests involving fist and elbow movements. During fist movement (Figure 8) at a frequency of 60 BPM, the F-PENG generated a voltage of 0.12 V. Similarly, for elbow movement (Figure 9) at the same tapping frequency, it produced a voltage of 0.43 V. The responses at both frequencies exhibit the same characteristic peaks for elbow bending, with higher voltage produced at higher frequencies, indicating that the PENG can detect both the movement and its intensity.

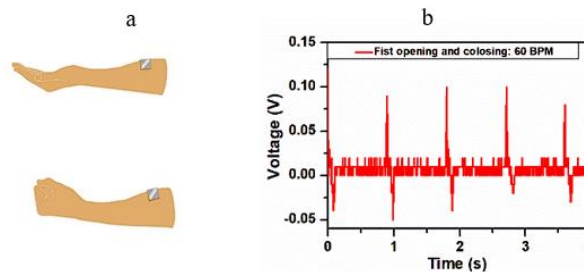


**Fig. 8:** Body Motion Sensing: Fist Movement.

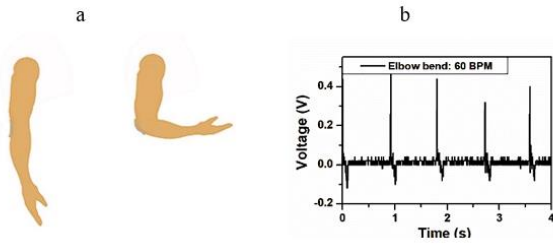


**Fig. 9:** Body Motion Sensing: Elbow Movement.

To further test the charging abilities of the PENG, it was installed between the two soles of a shoe to assess its performance during static jogging and running motions at 120 BPM and 240 BPM, respectively. The PENG's effectiveness in charging capacitors (Figure 10) of  $1\mu\text{F}$  and  $4.7\mu\text{F}$  was evaluated during these activities. The findings indicated that while jogging, the PENG charged the  $1\mu\text{F}$  and  $4.7\mu\text{F}$  capacitors to 0.9V and 0.55V, respectively, within 8 seconds. In running conditions, it charged the same capacitors to 1.1V and 0.67V, respectively, in the same duration. These results demonstrate the PENG's potential as a self-powered device for sensing pressure, force, and biomechanical motion.

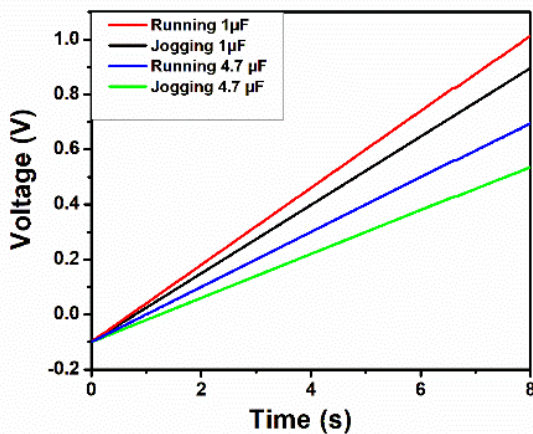


**Fig. 10:** Capacitor charging while jogging and running employing F-PENG.

To assess the energy harvesting and storage performance of the PENG, a circuit incorporating a full wave bridge rectifier was built and connected to capacitors, resistors, and LEDs (Figure 11). The capability of the PENG to charge capacitors with values of  $0.1\mu\text{F}$ ,  $1\mu\text{F}$ , and  $10\mu\text{F}$  was tested over a 12-second period at a tapping frequency of 180 BPM. The testing revealed that the  $0.1\mu\text{F}$  capacitor achieved a voltage of 6.3V, whereas the  $1\mu\text{F}$  and  $10\mu\text{F}$  capacitors reached 1.4V and 0.8V, respectively, with the lowest capacitance capacitor showing the highest voltage output, a result that aligns with the expectation of higher charge loss at greater capacitance. The charge and discharge behavior of the  $10\mu\text{F}$  capacitor was further examined, showing charge levels dependent on the force exerted on the PENG and discharge rates that were consistent, as determined by the capacitor's properties. Furthermore, the PENG successfully powered two LEDs after 30

seconds of tapping at 180 BPM, highlighting its effectiveness in energy harvesting and conversion.

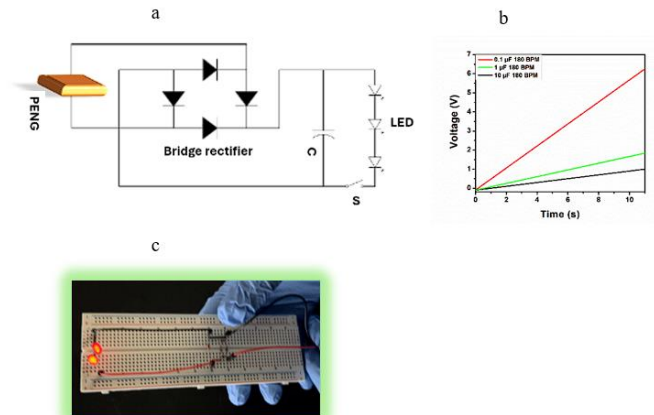


**Fig. 11:** (a) Circuit schematic of LED driving and capacitor charging from F-PENG, (b) Charging Different Capacitors for 12s at 180 BPM, (c) Driving the red LED by output power from beating PENG.

#### IV. CONCLUSION

In this research,  $\text{BaTiO}_3$  was successfully synthesized and integrated into a PDMS polymer matrix with MWCNTs, resulting in an effective piezoelectric energy harvester developed through a periodic mechanical beating process. The composite film PENGs, containing 40 wt.%  $\text{BaTiO}_3$  nanoparticles and 5 wt.% MWCNTs, generated a maximum output voltage of approximately 8 V. This output was sufficient to power two commercial red LEDs using a storage capacitor. Additionally, the device showed promising capabilities in self-powered force and biomechanical motion detection, presenting opportunities for cost-effective and easily manufacturable sensors. The energy-efficient production process used to transform nanorods into a composite film structure underlines the potential of  $\text{BaTiO}_3$  nanoparticle-based nanogenerators for energy harvesting and self-powered sensing applications.

#### REFERENCES

- [1] Wang X, Song J, Liu J, Wang ZL. Direct-current nanogenerator driven by ultrasonic waves. *Science*. 2007 Apr 6;316(5821):102-5.
- [2] Fan FR, Tian ZQ, Wang ZL. Flexible triboelectric generator. *Nano energy*. 2012 Mar 1;1(2):328-34.
- [3] Torres FG, De-la-Torre GE. Polysaccharide-based triboelectric nanogenerators: a review. *Carbohydrate Polymers*. 2021 Jan 1;251:117055.
- [4] Briscoe J, Dunn S. Piezoelectric nanogenerators—a review of nanostructured piezoelectric energy harvesters. *Nano Energy*. 2015 May 1;14:15-29.
- [5] Mahapatra B, Patel KK, Patel PK. A review on recent advancement in materials for piezoelectric/triboelectric nanogenerators. *Materials Today: Proceedings*. 2021 Jan 1;46:5523-9.
- [6] Nayak S, Chaki TK, Khashtgir D. Development of flexible piezoelectric poly (dimethylsiloxane)- $\text{BaTiO}_3$  nanocomposites for electrical energy harvesting. *Industrial & Engineering Chemistry Research*. 2014 Oct 1;53(39):14982-92.
- [7] Li GZ, Wang GG, Ye DM, Zhang XW, Lin ZQ, Zhou HL, Li F, Wang BL, Han JC. High-performance transparent and flexible triboelectric

- nanogenerators based on PDMS-PTFE composite films. *Advanced Electronic Materials*. 2019 Apr;5(4):1800846.
- [8] Ren X, Fan H, Zhao Y, Liu Z. Flexible lead-free BiFeO<sub>3</sub>/PDMS-based nanogenerator as piezoelectric energy harvester. *ACS applied materials & interfaces*. 2016 Oct 5;8(39):26190-7.
- [9] Zhang G, Liao Q, Zhang Z, Liang Q, Zhao Y, Zheng X, Zhang Y. Novel piezoelectric paper-based flexible nanogenerators composed of BaTiO<sub>3</sub> nanoparticles and bacterial cellulose. *Advanced Science*. 2016 Feb;3(2):1500257.
- [10] Sun QJ, Lei Y, Zhao XH, Han J, Cao R, Zhang J, Wu W, Heidari H, Li WJ, Sun Q, Roy VA. Scalable fabrication of hierarchically structured graphite/polydimethylsiloxane composite films for large-area triboelectric nanogenerators and self-powered tactile sensing. *Nano Energy*. 2021 Feb 1;80:105521.
- [11] Lin ZH, Yang Y, Wu JM, Liu Y, Zhang F, Wang ZL. BaTiO<sub>3</sub> nanotubes-based flexible and transparent nanogenerators. *The journal of physical chemistry letters*. 2012 Dec 6;3(23):3599-604.
- [12] F. Narita and M. Fox, "A Review on Piezoelectric, Magnetostrictive, and Magnetoelastic Materials and Device Technologies for Energy Harvesting Applications," *Adv Eng Mater*, vol. 20, no. 5, p. 1700743, May 2018, doi: 10.1002/adem.201700743.
- [13] J. Curie and P. Curie, "Développement par compression de l'électricité polaire dans les cristaux hémihédres à faces inclinées," *Bulletin de Minéralogie*, vol. 3, no. 4, pp. 90–93, 1880, doi: 10.3406/bulmi.1880.1564.
- [14] S. Katzir, "THE DISCOVERY OF THE PIEZOELECTRIC EFFECT," in *THE BEGINNINGS OF PIEZOELECTRICITY*, vol. 246, S. Katzir, Ed., in *BOSTON STUDIES IN PHILOSOPHY OF SCIENCE*, vol. 246, Dordrecht: Springer Netherlands, 2006, pp. 15–64. doi: 10.1007/978-1-4020-4670-4\_2.
- [15] H. S. Klickstein, "Pierre Curie—An appreciation of his scientific achievements," *J. Chem. Educ.*, vol. 24, no. 6, p. 278, Jun. 1947, doi: 10.1021/ed024p278.
- [16] W. P. Mason, "Piezoelectricity, its history and applications," *The Journal of the Acoustical Society of America*, vol. 70, no. 6, pp. 1561–1566, Dec. 1981, doi: 10.1121/1.387221.
- [17] I. Chinya, A. Pal, and S. Sen, "Polyglycolated zinc ferrite incorporated poly(vinylidene fluoride)(PVDF) composites with enhanced piezoelectric response," *Journal of Alloys and Compounds*, vol. 722, pp. 829–838, Oct. 2017, doi: 10.1016/j.jallcom.2017.06.028.
- [18] Z. L. Wang and J. Song, "Piezoelectric Nanogenerators Based on Zinc Oxide Nanowire Arrays," *Science*, vol. 312, no. 5771, pp. 242–246, Apr. 2006, doi: 10.1126/science.1124005.
- [19] Alluri, N. R.; Chandrasekhar, A.; Vivekananthan, V.; Purusothaman, Y.; Selvarajan, S.; Jeong, J. H.; Kim, S.-J. Scavenging biomechanical energy using high-performance, flexible BaTiO<sub>3</sub> nanocube/PDMS composite films. *ACS Sustainable Chem. Eng.* 2017, 5, 4730–4738, DOI: 10.1021/acssuschemeng.7b00117
- [20] Jian, G.; Jiao, Y.; Meng, Q.; Shao, H.; Wang, F.; Wei, Z. 3D BaTiO<sub>3</sub> flower based polymer composites exhibiting excellent piezoelectric energy harvesting properties. *Adv. Mater. Interfaces* 2020, 7, 2000484, DOI: 10.1002/admi.202000484
- [21] Alluri, N. R.; Saravanakumar, B.; Kim, S.-J. Flexible, hybrid piezoelectric film (BaTi<sub>1-x</sub>Zr<sub>x</sub>O<sub>3</sub>)/PVDF nanogenerator as a self-powered fluid velocity sensor. *ACS Appl. Mater. Interfaces* 2015, 7, 9831–9840, DOI: 10.1021/acsami.5b01760
- [22] Baek, C.; Wang, J. E.; Ryu, S.; Kim, J.-H.; Jeong, C. K.; Park, K.-I.; Kim, D. K. Facile hydrothermal synthesis of BaZr<sub>x</sub>Ti<sub>1-x</sub>O<sub>3</sub> nanoparticles and their application to a lead-free nanocomposite generator. *RSC Adv*. 2017, 7, 2851–2856, DOI: 10.1039/C6RA26285F
- [23] Yan, J.; Jeong, Y. G. Roles of carbon nanotube and BaTiO<sub>3</sub> nanofiber in the electrical, dielectric and piezoelectric properties of flexible nanocomposite generators. *Compos. Sci. Technol.* 2017, 144, 1–10, DOI: 10.1016/j.compscitech.2017.03.015
- [24] Luo, C.; Hu, S.; Xia, M.; Li, P.; Hu, J.; Li, G.; Jiang, H.; Zhang, W. A Flexible Lead-Free BaTiO<sub>3</sub>/PDMS/C Composite Nanogenerator as a Piezoelectric Energy Harvester. *Energy Technol.* 2018, 6, 922–927, DOI: 10.1002/ente.201700756
- [25] Wu, Y.; Ma, F.; Qu, J.; Luo, Y.; Lv, C.; Guo, Q.; Qi, T. Vertically-aligned lead-free BCTZY nanofibers with enhanced electrical properties for flexible piezoelectric nanogenerators. *Appl. Surf. Sci.* 2019, 469, 283–291, DOI: 10.1016/j.apsusc.2018.10.229
- [26] Park, K.-I.; Lee, M.; Liu, Y.; Moon, S.; Hwang, G.-T.; Zhu, G.; Kim, J. E.; Kim, S. O.; Kim, D. K.; Wang, Z. L. Flexible nanocomposite generator made of BaTiO<sub>3</sub> nanoparticles and graphitic carbons. *Adv. Mater.* 2012, 24, 2999–3004, DOI: 10.1002/adma.201200105
- [27] Tsege, E. L.; Kim, G. H.; Annapureddy, V.; Kim, B.; Kim, H.-K.; Hwang, Y.-H. A flexible lead-free piezoelectric nanogenerator based on vertically aligned BaTiO<sub>3</sub> nanotube arrays on a Ti-mesh substrate. *RSC Adv*. 2016, 6, 81426–81435, DOI: 10.1039/C6RA13482C
- [28] Zhang, G.; Zhao, P.; Zhang, X.; Han, K.; Zhao, T.; Zhang, Y.; Jeong, C. K.; Jiang, S.; Zhang, S.; Wang, Q. Flexible three-dimensional interconnected piezoelectric ceramic foam based composites for highly efficient concurrent mechanical and thermal energy harvesting. *Energy Environ. Sci.* 2018, 11, 2046–2056, DOI: 10.1039/C8EE00595H
- [29] Su, H.; Wang, X.; Li, C.; Wang, Z.; Wu, Y.; Zhang, J.; Zhang, Y.; Zhao, C.; Wu, J.; Zheng, H. Enhanced energy harvesting ability of polydimethylsiloxane-BaTiO<sub>3</sub>-based flexible piezoelectric nanogenerator for tactile imitation application. *Nano Energy* 2021, 83, 105809, DOI: 10.1016/j.nanoen.2021.105809
- [30] Zheng, Q.; Zhang, H.; Mi, H.; Cai, Z.; Ma, Z.; Gong, S. High-performance flexible piezoelectric nanogenerators consisting of porous cellulose nanofibril (CNF)/poly (dimethylsiloxane)(PDMS) aerogel films. *Nano Energy* 2016, 26, 504–512, DOI: 10.1016/j.nanoen.2016.06.009
- [31] Mao, Y.; Zhao, P.; McConohy, G.; Yang, H.; Tong, Y.; Wang, X. Sponge-like piezoelectric polymer films for scalable and integratable nanogenerators and self-powered electronic systems. *Adv. Energy Mater.* 2014, 4, 1301624, DOI: 10.1002/aenm.201301624
- [32] Sriphan, S.; Charoonsuk, T.; Maluangnon, T.; Vittayakorn, N. High-performance hybridized composited-based piezoelectric and triboelectric nanogenerators based on BaTiO<sub>3</sub>/PDMS composite film modified with TiO<sub>2</sub>. 802 nanosheets and silver nanopowders cofillers. *ACS Appl. Energy Mater.* 2019, 2, 3840–3850, DOI: 10.1021/acsaem.9b00513
- [33] Suo, G.; Yu, Y.; Zhang, Z.; Wang, S.; Zhao, P.; Li, J.; Wang, X. Piezoelectric and triboelectric dual effects in mechanical-energy harvesting using BaTiO<sub>3</sub>/polydimethylsiloxane composite film. *ACS Appl. Mater. Interfaces* 2016, 8, 34335–34341, DOI: 10.1021/acsami.6b11108
- [34] Hajra, S.; Padhan, A. M.; Sahu, M.; Alagarsamy, P.; Lee, K.; Kim, H. J. Lead-free flexible Bismuth Titanate-PDMS composites: A multifunctional colossal dielectric material for hybrid piezo-triboelectric nanogenerator to sustainably power portable electronics. *Nano Energy* 2021, 89, 106316, DOI: 10.1016/j.nanoen.2021.106316
- [35] Miranda I, Souza A, Sousa P, Ribeiro J, Castanheira EMS, Lima R, Minas G. Properties and Applications of PDMS for Biomedical Engineering: A Review. *J Funct Biomater*. 2021 Dec 21;13(1):2. doi: 10.3390/jfb13010002. PMID: 35076525; PMCID: PMC8788510.
- [36] C. Xu, C. Ouyang, R. Jia, Y. Li, and X. Wang, "Magnetic and optical properties of poly(vinylidene difluoride)/Fe<sub>3</sub>O<sub>4</sub> nanocomposite prepared by coprecipitation approach," *Journal of Applied Polymer Science*, vol. 111, no. 4, pp. 1763–1768, 2009, doi: 10.1002/app.29194.
- [37] O. D. Jayakumar, B. P. Mandal, J. Majeed, G. Lawes, R. Naik, and A. K. Tyagi, "Inorganic-organic multiferroic hybrid films of Fe<sub>3</sub>O<sub>4</sub> and PVDF with significant magneto-dielectric coupling," *J. Mater. Chem. C*, vol. 1, no. 23, pp. 3710–3715, May 2013, doi: 10.1039/C3TC30216D.
- [38] H. H. Singh, S. Singh, and N. Khare, "Design of flexible PVDF/NaNbO<sub>3</sub>/RGO nanogenerator and understanding the role of nanofillers in the output voltage signal," *Composites Science and Technology*, vol. 149, pp. 127–133, Sep. 2017, doi: 10.1016/j.compscitech.2017.06.013.
- [39] H. H. Singh, S. Singh, and N. Khare, "Design of flexible PVDF/NaNbO<sub>3</sub>/RGO nanogenerator and understanding the role of nanofillers in the output voltage signal," *Composites Science and Technology*, vol. 149, pp. 127–133, Sep. 2017, doi: 10.1016/j.compscitech.2017.06.013.
- [40] Z.-W. Ouyang, E.-C. Chen, and T.-M. Wu, "Enhanced piezoelectric and mechanical properties of electroactive polyvinylidene fluoride/iron oxide composites," *Materials Chemistry and Physics*, vol. 149–150, pp. 172–178, Jan. 2015, doi: 10.1016/j.matchemphys.2014.10.003.
- [41] S. K. Ghosh et al., "Yb<sup>3+</sup> assisted self-polarized PVDF based ferroelectric nanogenerator: A facile strategy of highly efficient mechanical energy harvester fabrication," *Nano Energy*, vol. 30, pp. 621–629, Dec. 2016, doi: 10.1016/j.nanoen.2016.10.042.

- [42] Meisak D, Kinka M, Plyushch A, Macutkevič J, Zarkov A, Schaefer S, Selskis A, Samulionis V, Kuzhir P, Banys JR, Fierro V, Celzard A. Piezoelectric Nanogenerators Based On BaTiO<sub>3</sub>/PDMS Composites for High-Frequency Applications. *ACS Omega*. 2023 Apr 6;8(15):13911-13919. doi: 10.1021/acsomega.3c00321. PMID: 37091415; PMCID: PMC10116497.
- [43] Bouhamed, A.; Jöhrmann, N.; Naifar, S.; Böhm, B.; Hellwig, O.; Wunderle, B.; Kanoun, O. Collaborative Filler Network for Enhancing the Performance of BaTiO<sub>3</sub>/PDMS Flexible Piezoelectric Polymer Composite Nanogenerators. *Sensors* 2022, 22, 4181. <https://doi.org/10.3390/s22114181>
- [44] C.-W. Tang, B. Li, L. Sun, B. Lively, and W.-H. Zhong, "The effects of nanofillers, stretching and recrystallization on microstructure, phase transformation and dielectric properties in PVDF nanocomposites," *European Polymer Journal*, vol. 48, no. 6, pp. 1062–1072, Jun. 2012, doi: 10.1016/j.eurpolymj.2012.04.002.
- [45] Y. Konishi and M. Cakmak, "Nanoparticle induced network self-assembly in polymer-carbon black composites," *Polymer*, vol. 47, no. 15, pp. 5371–5391, Jul. 2006, doi: 10.1016/j.polymer.2006.05.015.
- [46] O. Korostynska, K. Arshak, D. Morris, A. Arshak, and E. Jafer, "Radiation-induced changes in the electrical properties of carbon filled PVDF thick films," *Materials Science and Engineering: B*, vol. 141, no. 3, pp. 115–120, Aug. 2007, doi: 10.1016/j.mseb.2007.06.025.
- [47] S. L. Jiang et al., "Positive temperature coefficient properties of multiwall carbon nanotubes/poly(vinylidene fluoride) nanocomposites," *Journal of Applied Polymer Science*, vol. 116, no. 2, pp. 838–842, 2010, doi: 10.1002/app.31569.
- [48] G. Zhu, Z. Zeng, L. Zhang, and X. Yan, "Piezoelectricity in  $\beta$ -phase PVDF crystals: A molecular simulation study," *Computational Materials Science*, vol. 44, no. 2, pp. 224–229, Dec. 2008, doi: 10.1016/j.commatsci.2008.03.016.
- [49] S. Liu, S. Xue, W. Zhang, and J. Zhai, "Enhanced dielectric and energy storage density induced by surface-modified BaTiO<sub>3</sub> nanofibers in poly(vinylidene fluoride) nanocomposites," *Ceramics International*, vol. 40, no. 10, Part A, pp. 15633–15640, Dec. 2014, doi: 10.1016/j.ceramint.2014.07.083.
- [50] Luo C, Hu S, Xia M, Li P, Hu J, Li G, Jiang H, Zhang W. A flexible lead-free BaTiO<sub>3</sub>/PDMS/C composite nanogenerator as a piezoelectric energy harvester. *Energy Technology*. 2018 May;6(5):922-7.
- [51] Wang, H., Sun, X., Wang, Y. et al. Acid enhanced zipping effect to densify MWCNT packing for multifunctional MWCNT films with ultra-high electrical conductivity. *Nat Commun* 14, 380 (2023). <https://doi.org/10.1038/s41467-023-36082-2>.

#### AUTHORS

**First Author** – Islam Uddin Shipu, Master's in Chemistry, The University of Texas Rio Grande Valley, islamuddin.shipu01@utrgv.edu.

**Second Author** – Dipasree Bhowmick, Master's in Mechanical Engineering, The University of Texas Rio Grande Valley, dipasree.bhowmick01@utrgv.edu.

**Third Author** – Nondon Lal Dey, Master's in Physics, University of Louisiana at Lafayette, nondon.deyl@louisiana.edu

**Correspondence Author** – Islam Uddin Shipu, islamshipu68@gmail.com, +1 956 598 1703.